PROBABILISTIC METHODS FOR STRUCTURAL DESIGN AND RELIABILITY

Christos C. Chamis
National Aeronautics and Space Administration
Glenn Research Center
Cleveland, Ohio 44135

ABSTRACT

This report describes a formal method to quantify structural damage tolerance and reliability in the presence of a multitude of uncertainties in turbine engine components. The method is based at the material behavior level where primitive variables with their respective scatter ranges are used to describe behavior. Computational simulation is then used to propagate the uncertainties to the structural scale where damage tolerance and reliability are usually specified. Several sample cases are described to illustrate the effectiveness, versatility, and maturity of the method. Typical results from this method demonstrate that it is mature and that it can be used to probabilistically evaluate turbine engine structural components. It may be inferred from the results that the method is suitable for probabilistically predicting the remaining life in aging or deteriorating structures, for making strategic projections and plans, and for achieving better, cheaper, faster products that give competitive advantages in world markets.

INTRODUCTION

Achieving and retaining competitive advantages in world markets necessarily leads to proactive drives for getting better, cheaper, faster products to market, a phenomenon that becomes even more important in the high-tech sector including aerospace vehicles. The awareness for natural resource conservation also leads to the cost-effective useful life extension of existing products. These activities require that we effectively use available resources and that we formulate methods to quantify the current strength of a specific structure or component and reliably evaluate its remaining strength and/or life. A multitude of uncertainties must be dealt with to meet these requirements: new, unproven methods for design and manufacturing; a lack of sufficient data on new candidate materials; unknown assumptions and conditions related to the initial design; records of environmental exposure; and material degradation from various factors.

With respect to the aforementioned uncertainties, probabilistic methods offer formal approaches to quantify those uncertainties and to evaluate their effects on material behavior, on service, and on attendant reliabilities and risks. The objective of this report is to describe one probabilistic method used to evaluate the effects of uncertainties on structural damage tolerance and reliability from material behavior to service life and to retirement for cause. The probabilistic method is based on formulations that describe the physics in terms of primitive variables and respective scatter ranges at the lowest engineering manageable scale and at all subsequent scales up to the highest where reliability is evaluated. The method relies on computational simulation to propagate uncertainties from the elementary scale and all intermediate scales where the probabilistic evaluation and reliability of specific responses are needed. The method has evolved over the past 15 years and has matured sufficiently to evaluate structural damage tolerance and reliability under various scenarios [Refs. 1 to 3]. It has several unique features, two of which are the most useful for presenting results: (1) quantifiable reliability in terms of cumulative

distribution functions and (2) sensitivity factors of the primitive variables that affect that reliability.

This report begins with an introduction of the fundamental concept and computational simulation methods and gives a simple example. Next is a brief description of the method and its attendant computer codes. Several sample cases are then discussed to (1) illustrate its versatility, (2) present the large amounts of information generated, (3) show the relevance of the information, and (4) make recommendations concerning design, material development quality, certification, in-service health monitoring, retirement for cause, and recycling. The description is limited to typical results obtained and their respective interpretations. References are cited for specific details.

FUNDAMENTAL CONCEPTS

The following simple example describes some fundamental concepts of probabilistic structural analysis and design: the probabilistic evaluation of the tip displacement of a cantilever beam loaded at the free end as shown schematically in Figure 1(a). The equation (deterministic model) for predicting the tip displacement is

$$w = \frac{4Pl^3}{Ebt^3} \tag{1}$$

where w is the response variable, P is the load, l is the length, E is the material stiffness, b is the width, and t is the thickness. This equation describes the physics of the response sought and includes the fundamental parameters (primitive variables) that govern the tip displacement. These primitive variables can also be grouped in three generic categories: load (P), geometry (l, b, and t), material (E). If we make several cantilever specimens, there will probably be some scatter of values for each of the primitive variables. Therefore, the task of probabilistic simulation is to account for the effects of that scatter on the displacement of the beam.

The task is considerably simplified when we recognize that (1) the tip displacement equation is the analog of the physical testing machine and (2) the scatter range in the primitive variables, P, l, b, t, and E, can be assumed to be represented by simple, well-known statistical distributions (Figure 1(b)), which will be helpful in simulating the effects of scatter on beam displacement. The following procedure is used to evaluate the effects of the uncertainties of the primitive variables on the tip displacement:

1. Decide the range of the scatter in each primitive variable. This range in practical cases is established from experience but for this example, assume that scatter is about ±5 percent from the assumed mean value. The scatter for the modulus is between 24 and 28 mpsi; for the length, between 19 and 21 in.; for the width, between 0.95 and 1.05 in.; for the thickness, 1.20 and 1.30 in.; and for the load, between 80 and 120 lb. It is important to note that the only test data available were the mean values for the primitive variables. The range of the scatter was assumed for reasons that will become clear later. Note that the mean value for each primitive variable with a truncated distribution generally is where the vertical line (drawn from the peak of the respective distribution) intersects the horizontal line.

2. Randomly select for each primitive variable in the equation a value from within its respective distribution. Having the simple statistical distributions allows nonbiased random selections to

be made. For example, the values selected randomly can be 25.5 mpsi for E; 20.8 in. for l; 0.99 in. for b; 1.27 in. for t; and 115 lb for P.

3. Substitute the randomly selected values in the equation to obtain 0.08 in. for the tip displacement.

4. Repeat step 3 for different sets of primitive variable values until sufficient data (as described subsequently) have been accumulated to plot the probability distribution curve (Figure 1(c)). For example, the mean value will be close to 0.065 in. There is about a 95-percent probability from the cumulative probability curve (Fig. 1(c)) that the tip displacement will be less than 0.08 in., or 95 of 100 trial calculations in step 3.

The generation of the data as described in step 4 is called a direct Monte Carlo simulation and generally requires a large number of simulations (tens of thousands). Methods and algorithms have been developed to generate the two probability graphs for the displacement with relatively few simulations, which for the first-order reliability method (FORM) is $2n+1$, where n is the number of primitive variables with scatter ranges. One such method, the fast probability integration (FPI), [Ref. 3], was used to generate the probability curve of figure 1(c). The application of FPI requires inputs of the mean value, scatter range, and the known or assumed probability density function of the scatter for each participating primitive variable. It becomes evident that the probabilistic simulation can be performed with known mean values, judiciously assumed scatter ranges, and respective distributions for the primitive variables.

A byproduct of the FPI is the sensitivity factors (Figure 1(d)). These factors probabilistically quantify and order the sensitivity of the cumulative distribution function of the response variable (displacement) to the uncertainty (scatter range) in the primitive variables (material, geometry, loads). For this example, the load (primitive variable) has about the same effect on the tip displacement (response variable) as the geometry parameters (primitive variables) at a low probability (<1 in 1000) whereas the thickness (primitive variable) dominates at high probabilities (>999 in 1000). Sensitivities are discussed in the following sections. For application to structural components or systems, the foregoing method using FPI is generalized as follows:

1. Develop or use a deterministic model for the entire component or system with its boundary, load, and expected environmental conditions. Practical structural situations would dictate that this be predominately a finite-element model.

2. Identify the primitive variables in the deterministic model. These will include material properties, fabrication process variables (pressure, temperature, and other loading conditions), structural parameters, loads (including environment), boundary conditions, and so forth. For composite structures, use integrated composite mechanics to predict the composite properties, beginning with micromechanics and accounting for both fabrication and environmental effects.
3. Obtain or assume mean values, scatter range, and probabilistic distribution (density function and standard deviations) for each primitive variable.

4. Perturb each primitive variable on either side of its respective means by a reasonably small amount (usually up to 10 percent) as a ratio of the respective standard deviation (up to 20 percent may be used, but with caution). Any amount greater than 20 percent may be more a

shift or even multimodal instead of reasonable scatter. Amounts greater than 20 percent would indicate that the input data might represent more than one population.

5. Conduct deterministic analyses with the values selected in step 4.

6. Repeat steps 4 and 5 several times ($2n$ + 1 for FORM) to generate sufficient information for FPI use.

7. Use FPI to generate the probability distribution functions for the desired responses, displacement, stress, and frequency and for the respective sensitivities at select probability levels. Recall that the number of perturbations usually needed with FPI is $2n+1$, where n is the number of primitive variables and 1 is using only their means in the same simulation run.

The above generalized method is practical through the use of computer codes to be described subsequently, and it is applicable to almost all disciplines and structures described herein.

PROBABILISTIC SIMULATION OF COMPONENTS AND SYSTEM RELIABILITY

To evaluate turbine engine component and system durability and reliability, probabilistic simulations must be performed for the loading conditions, the structural components, including supports, and the material(s) behavior. Each of the simulations must be defined by inputs of its respective deterministic model, primitive variables, and their attendant scatter range. The probabilistic simulation proceeds to evaluate a specific response and its scatter. The evaluated response is then compared with the corresponding resistance to assess the probability of failure, which can be used later to evaluate component and system durability and reliability. Figure 2, a conceptual schematic of the procedure, shows the three essential parts of component and system reliability simulation; the structural response obtained; the resistance evaluated; the probable damage (overlap of response scatter with resistance scatter); the information passed on for reliability and risk assessments; and the institutions that participated to develop the requisite formalism and then implemented it in an operational computational procedure [Ref. 1]. A block diagram of the computer code logic is shown in Figure 3.

The schematics in Figures 2 and 3 summarize probabilistic structural performance assessment. The concept is relatively straightforward and appears simple; however, implementation in a workable computer code requires knowledge of advanced structural mechanics, efficient probabilistic algorithms, material behavior, and proficient and subtle computer programming techniques.

In Figure 3, note that uncertainties in the human factor and the computer code can also be included; inputs for required performance, component and system longevity, and acceptable reliability and risk must be provided; and the simulation provides information to probabilistically select verification tests to assure component and system certification with an acceptable reliability and an affordable risk. These will now be described.

Simple loading conditions can be input directly to the probabilistic structural analysis. Complex loading conditions require system-specific computer codes. Those for the space shuttle main engine are simulated by the composite load spectra computer code [Ref. 2]. Probabilistic structural analysis is performed by a specialty computer code [Refs. 2 and 3].

PROBABILISTIC SIMULATION OF MATERIAL BEHAVIOR

Developed at the Glenn Research Center, the probabilistic simulation of material behavior is relatively new and as far as the author knows, is the only one of its kind. Since the subject of this report is durability and reliability, materials-based life prediction is an important part. Therefore, the probabilistic material behavior models (PMBM) used in the simulation will be described in detail. The deterministic model evolved during research on high-temperature metal matrix composites (Ref. 4). Implementing the deterministic model for probabilistic simulations was funded from a research grant with the objective of formally describing uncertainties in material behavior for space shuttle main engine components [Ref. 5].

Conceptually, the model is based on the self-evident axiom that each material characteristic property observed by conventional testing constitutes a multidimensional surface. That surface is described by a multidimensional vector for which each component represents one observed or assumed effect (temperature, stress, time, etc.) on that material characteristic property. The surface is represented by a respective multifactor model of product form. The product form is assumed to conveniently represent mutual interactions among the various factors. Each factor consists of four different variables or parameters: (1) a terminal or final value, (2) a reference value, (3) a current value, and (4) an exponent. The exponent is selected to represent continuous monatomic behavior so that the factor equals unity when the current value equals the reference value and approaches either zero or infinity (depending on the specific behavior of the factors) when the current value approaches the final value. A schematic for a unit cell of material is shown in Figure 4 for composites and homogeneous materials. In equation form, the model is represented as

$$\frac{P}{P_o}=\left(\frac{T_F-T}{T_F-T_o}\right)^i\left(\frac{S_F-\sigma}{S_F-\sigma_o}\right)^l\left(\frac{\dot{S}_F-\dot{\sigma}}{\dot{S}_F-\dot{\sigma}_o}\right)^m \times\left(\frac{\dot{T}_F-\dot{\sigma}}{\dot{T}_F-\dot{\sigma}_o}\right)^n\left(\frac{R_F-R}{R_F-R_o}\right)^p\left(1-\frac{\sigma_M N_m}{S_F N_{MF}}\right)^r \times\left(1-\frac{\sigma_T N_T}{S_F N_{TF}}\right)^s\left(1-\frac{\sigma_t}{S_F t_F}\right)^u \cdots \tag{2}$$

where

P	property
T	temperature
S	strength
R	metallurgical reaction
N	number of cycles
t	time
σ	stress

and the subscripts are o, reference; F, final; M, mechanical; and T, thermal. The over dot signifies the rate.

To summarize, the multifactor interaction model provides the following:

- Gradual effects during most of the range, rapidly degrading near final stages
- Representation of the in situ behavior for fiber, matrix, interphase, and coating
- Introduction of primitive variables
- Consistent representation of all in situ constituent properties in terms of primitive variables
- Room-temperature values for reference properties
- Continuous interphase growth
- Simultaneous interaction of all primitive variables
- Adaptability to new materials
- Amenability to verification inclusive of all properties
- Adaptability to incremental computational simulation

Probabilistic results from the model [Ref. 5] are shown in Figure 5 where the cumulative distribution function curves for lifetime strengths are given for three temperatures. The curves shift to the left and their scatter range increases slightly with increasing temperature, as physically would be expected. One can infer from these curves that the MFIM could be used in conjunction with selective testing to substantially reduce the number of tests and the amount of time required to characterize material behavior in complex environments. Note that the MFIM is not restricted to the use just described but is generic in that each factor can be further substructured to another set of factors which may influence a specific factor (i.e., alloying elements, processing conditions, tolerance, assembly misfits, etc.). This generic use is discussed in Reference 6, which describes its application to simulate the effects of the human factor in structural analysis. Analogously, the MFIM can be used for evaluating aging effects on material deterioration simply by including deterioration factors.

DEMONSTRATION CASES

Two-Stage Rotor

This case demonstrates one direct way to evaluate component and system reliability under multiple failure modes. A schematic of the rotor with a summary of the results is shown in Figure 6. The details of this case are described in Reference 7, but this report will discuss the significance of the results and the respective sensitivity factors. Four failure modes were evaluated as noted in Figure 6. The survival probability of the rotor for each failure mode and the combination of failure modes are determined from a special plot of survival probability versus remaining resistance. This plot graphically depicts the critical failure mode and the system failure mode. As can be seen, the critical failure mode is fracture at the rim in 10 000 cycles, which coincides with the system failure mode. Also seen is that when the burst failure mode has 100 percent survival probability, the system has only about 65 percent. Table I lists the sensitivity factors that influence system failure. The left column gives the primitive variables included in the evaluations, and the right column gives the magnitude of each factor's contribution to the system probability of failure or reliability. These sensitivity magnitudes are part of the probabilistic simulation from using FPI and are evaluated simultaneously with the probability, as mentioned in the cantilever example in the section Fundamental Concepts. One may observe from this table that the four most dominant factors (in order of magnitude) are rotor speed, density, temperature, and crack growth constant C. The remaining factors make negligible contributions. For example, critical parameters in damage tolerance evaluations (initial crack size A_0 and constants C in the fracture mode, N_i and K_t) are insignificant in the rotor reliability assessment. The only critical material property is the rotor density. Therefore, recommendations

for rotor material suppliers are that they control the scatter of the rotor material density and the thermal expansion coefficient. Also, rotor designers must assure that the rotor does not over-speed, that expected temperature spikes be accounted for, and that unexpected hot spots be avoided. This probabilistic evaluation of the rotor illustrates that probabilistic results can be used to provide guidelines for material quality control and design considerations, both of which are essential in product safety, reliability, and cost reduction.

Combustor Liner

The engine combustor liner to be described could be a part for a supersonic aircraft engine. As a result of the combustion process, the liner is subjected primarily to thermal loads and to some pressure. Figure 7 shows the finite-element model of the liner and the thermal loading profile along the combustor. The details of this evaluation are described in Reference 8. For this discussion, assume that the liner is constructed of a cross-ply (woven fabric) ceramic matrix composite and that it is designed for the avoidance of vibration frequencies and buckling. The probabilistic results are presented and the usage of these results for damage tolerance and reliability of the combustor liner are described. Guidelines and recommendations for material selection may be obtained from the sensitivity factors.

The cumulative distribution function of the first (lowest) vibration frequency is shown in Figure 8(a). This frequency has a mean of 320 cycles/sec and a scatter range from 290 to 350 Hz, about 60 Hz. The sensitivity factors for two levels of probability are shown in Figure 8(b). Evident from figure 8(b) is that liner material density and shear modulus have a significant effect on the liner frequency; the liner thickness has the dominant effect and is even more dominant at higher probability values; and the order of the sensitivity factors is the same at low and high probability values.

The cumulative distribution function for buckling of the liner is shown in Figure 9(a) and the respective sensitivities are shown in Figure 9(b). The mean value of the buckling pressure is six times that of the operating pressure, or 60 psi. The attendant scatter range is from about 45 to 75 psi. The reliability of the liner for buckling is 100 percent with no risk since the applied mean pressure is only 10 psi, or 6.5σ away from probable overlap. The factors that exert the greatest influence on the buckling load are the liner thickness (geometry variable), thermal expansion coefficient (material variable), and thermal load (loading conditions of 2150 °F). The material moduli (axial, hoop, and shear) have a negligible effect. Note that the order of the sensitivities remains the same for low and high probability values, which means that the buckling load probability is linear throughout the scatter range of each primitive variable. On the basis of these results, the recommendation for material suppliers is that they control the thermal expansion coefficient. For designers, it is recommended that they control the temperature, select the liner thickness to assure that it will survive at least 4.5 times the operating pressure, and specify proof test pressures of at least 7.5 times the operating pressure to assure that the liner will buckle in the first test to verify the simulation results.

Space Shuttle Main Engine (SSME) High-Pressure Blades

The space shuttle main engine blades are in the liquid hydrogen pump, are relatively small, rotate at about 40 rpm, and are subjected cyclically to very cold and very high temperatures (thermomechanical fatigue). The blade airfoil with its respective operating loading conditions

and finite-element model are shown in Figure 10. The blade has relatively steep spanwise thermal and pressure gradients.

The cyclic temperature and load effects on the blade materials were simulated by the MFIM described previously (fig. 4). The specific values for the various factors used are listed in Table II. Note that four factors were sufficient for that simulation: (1) the temperature dependence with an exponent of 1/2; (2) the stress dependence with exponent n; (3) the pressure cyclic load with exponent p; and (4) the thermal cyclic load with exponent q. The temperature effects exponent was assumed to be a constant based on previous studies whereas exponents n, p, and q were assumed to have the scatter shown in Table II.

The damage propagation path caused by 100 000 fatigue cycles is shown in Figure 11 for two probability levels (1/100 000 and 2/10 000). Obviously, the path with the highest probability will most likely occur first. It is noted that several other paths are probable with probability levels between the two shown in Figure 11. However, none was found with a higher probability than (2/10 000). The durability, or damage tolerance, of the blade in its operating environment can be simulated by using progressive structural fracture [Ref. 9]. This approach requires neither fine finite-element meshes nor traditional fracture toughness parameters. The results for the strain energy release rate versus the damage state are plotted in Figure 12. The two major points worth noting in Figure 12 are that the damage is stable and progresses rather slowly up to damage state 3, and the damage progression increases very rapidly from damage state 3 to damage state 4. The plot in this figure displays several important aspects of structural durability and/or damage tolerance:

- The blade is damage tolerant up to damage state 3.
- With continuing operation, the blade will fracture (disintegrate) just past damage state 4.
- The safe design of the blade with 100-percent reliability is up to damage state 2.
- The blade should be inspected for damage states 1 and 2.
- At damage state 2, the blade must be replaced (retired for cause) to ensure safe operation of the SSME.
- Rather than inspect the blade, a costly and time-consuming task, in-service health should be monitored based on changes in select blade responses (e.g., vibration frequencies and vibration mode shapes) to indicate the damage state.

An important observation from the previous discussion is that an abundance of information generated by probabilistic computational simulation can be judiciously used from conceptual design to retirement for cause (from cradle to grave). Also, plots comparable to Figure 12 can be made for other responses (e.g., blade material degradation due to oxidation or other causes) provided that appropriate factors are used in the MFIM.

The information from Figure 12 can be combined with costs for fabrication and failure (penalties). The results are shown in Figure 13 as log-log plots for probability of damage initiation versus number of cycles and for total cost versus fatigue cycles. Note that the cost increases very rapidly with fatigue cycles higher than 10 000. Interestingly, the information in Figure 13 is really the cascading type because it can also be used to generate information for benefits accrued by improving material strength or controlling the quality of processing. Costs to improve structural reliability by decreasing scatter are more beneficial than costs to increase strength for comparable probabilities in general (unpublished in-house results by the author and his collaborators).

FAULT TREE SIMULATION FOR SYSTEM RELIABILITY

Systems usually fail by combinations of multiple failure modes. Multiple failure mode reliability is evaluated by a formal combination of the probability of failure of each failure mode. Traditionally, the formal method for combining those probabilities has been the fault tree simulation. Figure 14 schematically depicts a fault tree simulation for the SSME high-pressure blade. The evaluation includes four failure modes, the probability of failure for each being determined by probabilistic structural analysis. The modes are then combined by classical probability methods. The details of this process are described in Reference 10. Herein, we present some typical results and discuss their significance to material behavior and its influence on structural system reliability. The parameters (primitive variables) with their respective scatter standard deviation and assumed distributions included in the simulation are listed in Table III. Results obtained for the probability of system failure are shown in Figure 15. The probability for system failure from each individual failure mode is shown in Figure 15(a) with the simulated correlation coefficients for the three failure modes. From Figure 15(a), the system is predicted to fail by creep (stress rupture) because that failure mode has the highest probability of failure. Also, the stress influences the vibration failure mode and the creep failure mode significantly, even though the system failure probability from stress only is relatively small as compared with the other two. The sensitivity factors for system failure probability are shown in Figure 15(b). The dominant factor is the direction solidification angle θ_y measured from the blade radial (spanwise) axis. The modulus and the Poisson's ratio have about the same influence, but the rest have relatively negligible influence. Recommendations for materials suppliers and designers are comparable to those mentioned previously. Recommendations for the blade manufacturers and the rotor assembler are that they assure that the blade solidification direction line up with the blade spanwise axis. Important from the previous discussion is that system reliability can be formally evaluated for multiple failure modes. The critical failure modes are identifiable and their respective dominant sensitivities are quantifiable.

Three approaches were described for evaluating system reliabilities. The first is summarized in Figure 6, the second in Figures 11 and 12, and the third in Figures 13 and 14, all with their attendant discussions. The first and second methods are evaluated directly from the probabilistic structural and stress analysis, whereas the third requires fault tree evaluation in addition to probabilistic structural and stress analyses. The computer code described in Reference 3 was used for all three approaches.

CONCLUDING REMARKS

A formal method to quantify structural damage tolerance and reliability in the presence of a multitude of uncertainties in turbine engine components is described. The results of using probabilistic methods to predict structural damage tolerance and reliability from materials to service environments lead to the following remarks:

1. Probabilistic methods via computational simulation can be adapted throughout the structural design practice. They provide quantifiable information that can be used to reduce the costs of product development, certification, and risk.

2. These methods constitute a virtual statistical desktop laboratory applicable at all stages and for all aspects of the following: design, material selection and qualification, development, certification, and service life cycles.

3. Probabilistic methods rely on computational simulation results and are primarily useful for decision making, especially in the preliminary design stages.

4. Probabilistic methods provide a significant infrastructure that can be used to make predictions for future strategic projections and planning to assure better, cheaper, faster products that will give competitive advantages. These methods also have acceptable reliability, quantifiable risk, and capability to evaluate the remaining life of existing products.

REFERENCES

1. Chamis, C.C.: Probabilistic Structural Analysis Methods for Space Propulsion System Components. Probabilistic Engineering Mechanics, 1987, vol. 2, pp. 100–110.
2. Ho, H.W.; and Newell, J.F.: Composite Load Spectra for Select Space Propulsion Structural Components. Final Report, NASA CR–194476, 1994.
3. Probabilistic Structural Analysis Methods (PSAM) for Select Space Propulsion Systems Components: Part 2. Topical Annual Report, no. 6, NASA CR–187200, 1991.
4. Chamis, C.C. and Hopkins, D.A.: Thermoviscoplastic Nonlinear Constitutive Relationships for Structural Analysis of High Temperature Metal Matrix Composites. NASA TM–87291, 1985.
5. Scheidt Bast, C.C.: Probabilistic Material Strength Degradation Model for Inconel 718 Components Subjected to High Temperature, Mechanical Fatigue, Creep and Thermal Fatigue Effects. NASA CR–195284, 1994.
6. Chamis, C.C. and Singhal, S.N.: Probabilistic Simulation of the Human Factor in Structural Reliability. NASA TM–106498, 1994.
7. Mahadevan, S. and Chamis, C.C.: Structural System Reliability Under Multiple Failure Modes. AIAA Paper No. 93–1379, 1993, pp. 707–713.
8. Pai, S.S. and Chamis, C.C.: Probabilistic Assessment of Combustor Liner Design. ASME Paper No. 95–GT–121, 1994.
9. Chamis, C.C., Murthy, P.L.N. and Minnetyan, L.: Progressive Fracture in Composite Structures. ASTM STP–1285, 1997, pp. 70–84.
10. Torng, T.Y., Wu, Y.-T. and Millwater, H.R.: Structural System Reliability Calculation Using Probabilistic Fault Tree Analysis Method. AIAA Paper No. 92–2410, 1992, pp. 603–613.

TABLE I.—ROTOR SYSTEM RELIABILITY SENSITIVITY FACTORS AT 1/1000 PROBABILITY

SPEED	0.850827
ROTOR DENS	.438499
TEMPE	.170793
C	.133702
RINGY	.073086
RK1C	.061872
Kt	.060917
AO	.057976
E_ROT	.016011
BURST	.011983
A_LCF	.005132
E_RIN	.002698
NI	.000386
RING DENS	.000008
TOLER	0

TABLE II.—MULTIFACTOR INTERACTION MODEL VALUES USED IN PROBABILISTIC SIMULATION OF MATERIAL BEHAVIOR OF HIGH-PRESSURE BLADE OF SPACE SHUTTLE MAIN ENGINE

Variable	Distribution type	Mean	Standard deviation	
			Value	Percent of mean
Temperature, °F				
Final, T_F	Normal	2750	51.4	2.0
Initial, T_0,	Normal	68	2.04	3.0
Final strength, S_F, ksi	Normal	212.0	10.6	5.0
Initial stress, σ_0	Constant	0	0	0
Number of mechanical cycles				
Final, N_{MF}	Lognormal	10^8	5×10^6	5.0
Initial, N_{M0}	Lognormal	10^3	50	5.0
Number of primitive variables with scatter ranges, n	Normal	0.25		3.0
Exponent for pressure cyclic load, p	Normal	.25		3.0
Exponent for thermal cyclic load, q	Normal	.25		3.0

TABLE III.—PRIMITIVE VARIABLES USED IN FAULT TREE SIMULATION FOR SYSTEM RELIABILITY

	Mean[a]	Standard deviation	Distribution	Bottom event
Material orientation				
θ_x	0.05236	0.067544	Normal	All
θ_y	−.03491	.067544	Normal	All
θ_z	.08727	.067544	Normal	All
Modulus				
Elastic, E_0[a]	18.36×10^6	$.44595\times10^6$	Normal	All
Shear, G_0[a]	18.63×10^6	$.4657\times10^6$	Normal	All
Poisson's ratio, ν_0[a]	.386	.00965	Normal	All
Creep equation coefficient, B_0	86.0	.086	Normal	Creep
Density, ρ	$.805\times10^{-3}$	$.493\times10^5$	Normal	Frequency

[a]Defined at room temperature.

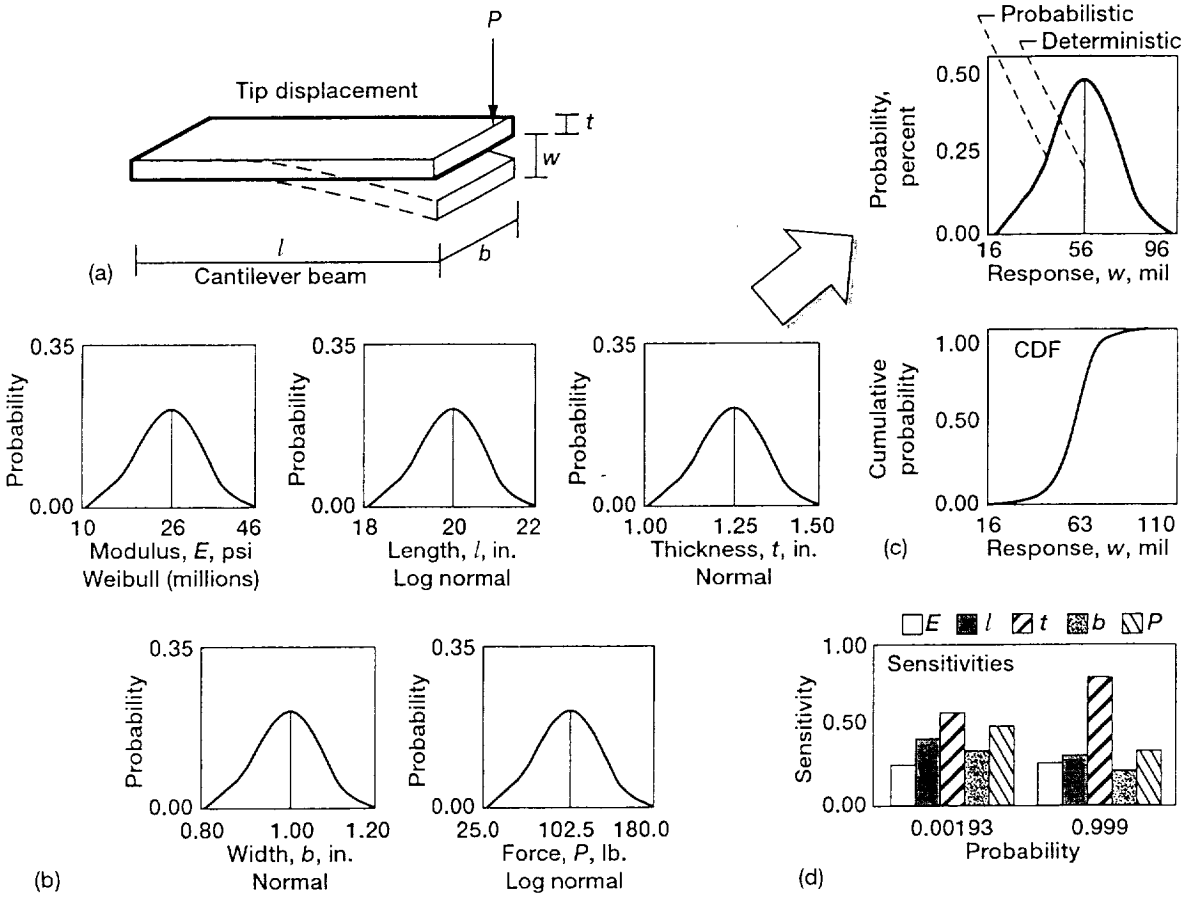

Figure 1.—Probabilistic structural analysis and response, (a) Structural analysis model. (b) Distribution of primitive variables P, l, E, t, b. (c) Distribution of response variables w. (d) Sensitivity factors.

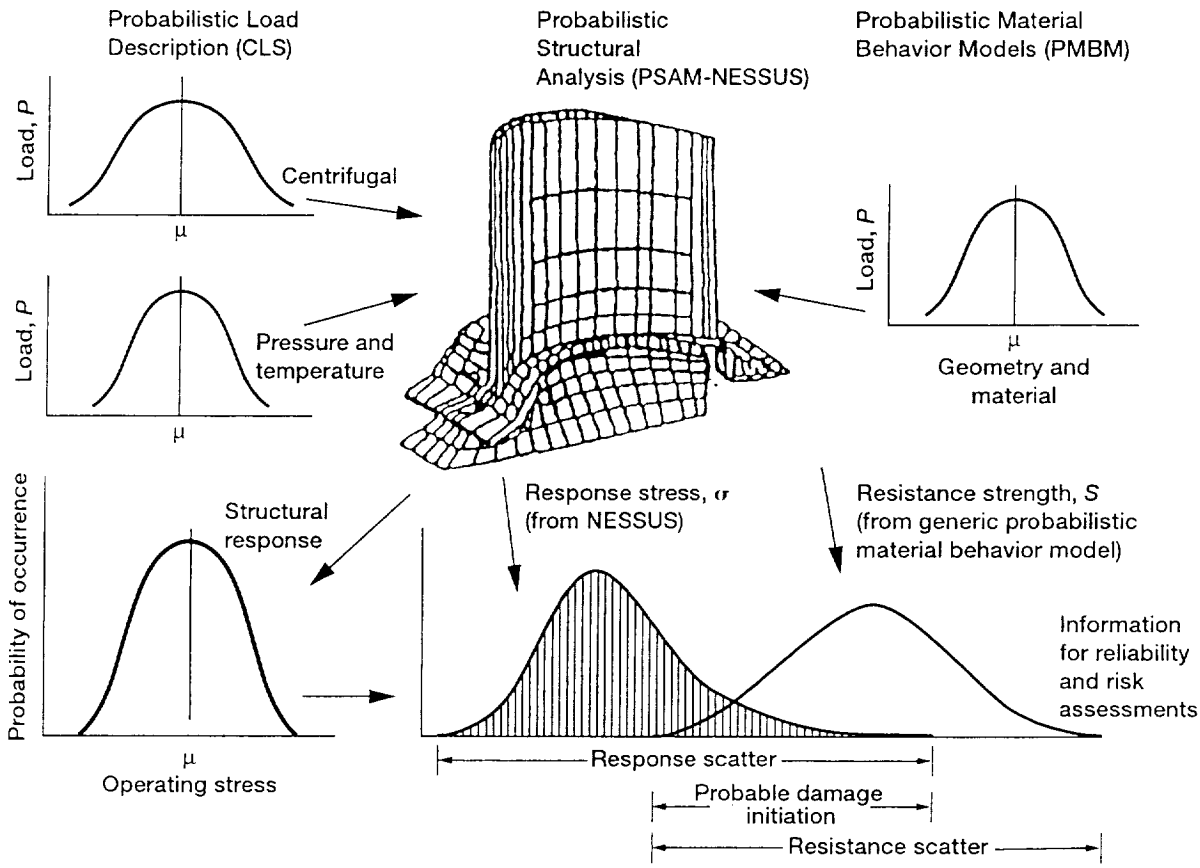

Figure 2.—Concept of probabilistic structure and component reliability.

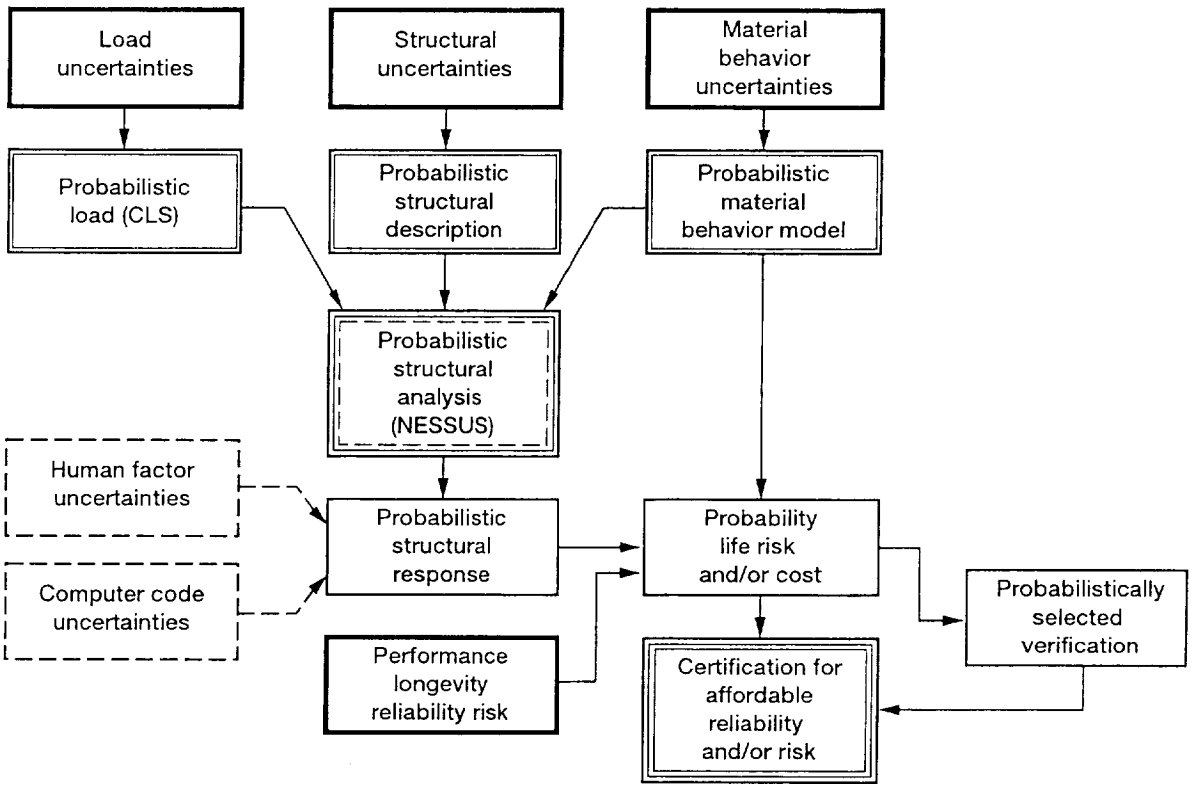

Figure 3.—Probabilistic structural simulation for assured certification.

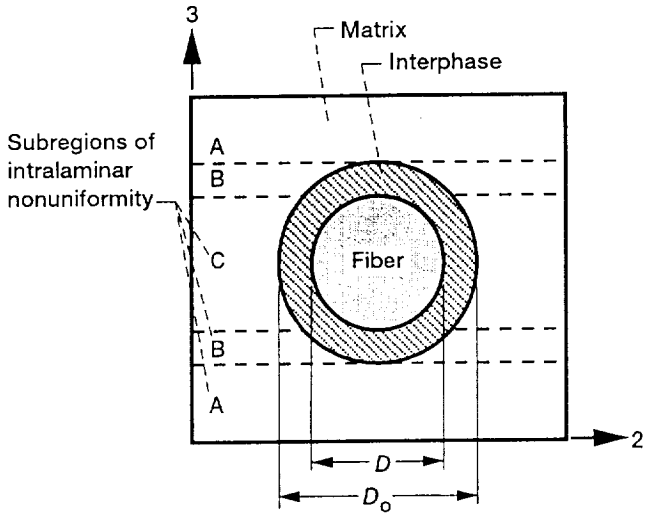

Figure 4.—Concept of unit cell of material behavior through multifactor interaction model (MFIM).

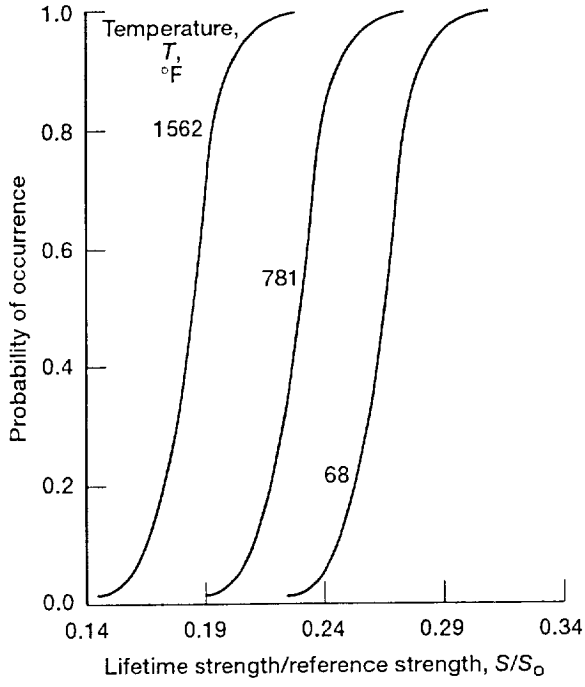

Figure 5.—Probabilistic material behavior model (PMBM) simulated lifetime strength for nickel-based superalloy subjected to 3162 stress cycles and 100 hr of creep.

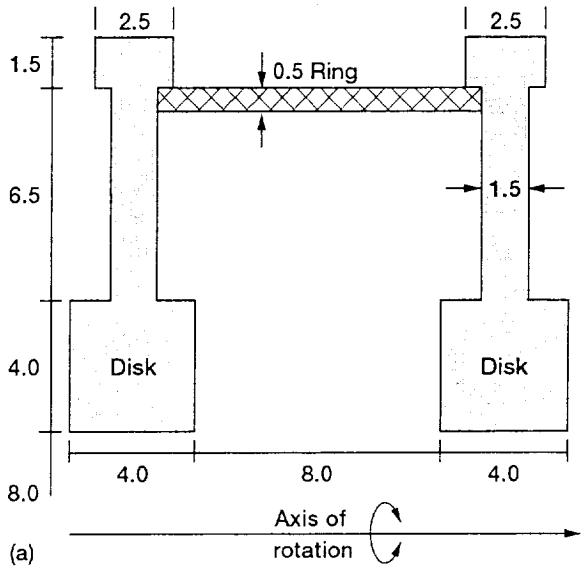

Figure 6.—Structural system reliability of two-stage rotor with multiple failure modes. (a) Rotor system. (b) Critical failure mode and system failure mode. All dimensions are in inches.

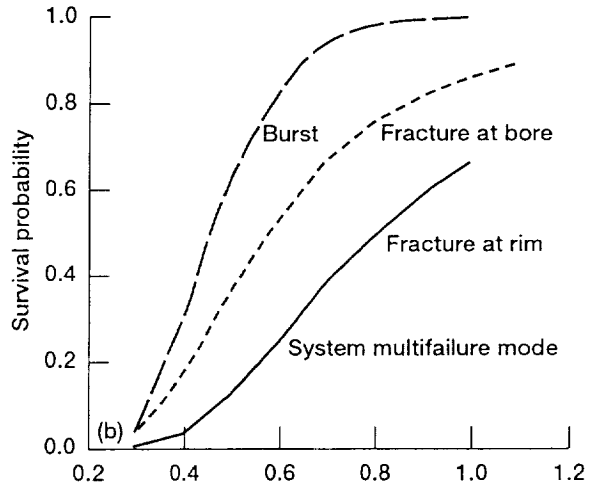

Failure mode	Applied stress	Resistance
1. Disk burst	Average stress	Burst strength
2. Fracture at bore	Fracture life	10 000 cycles
3. Fracture at rim	Fracture life	10 000 cycles
4. Progressive damage	Yielding of ring[a]	Yield strength

[a]Yielding of ring affects all other modes through mutual interaction.

Figure 6.—Concluded. (b) Critical failure mode and system failure mode. All dimensions are in inches.

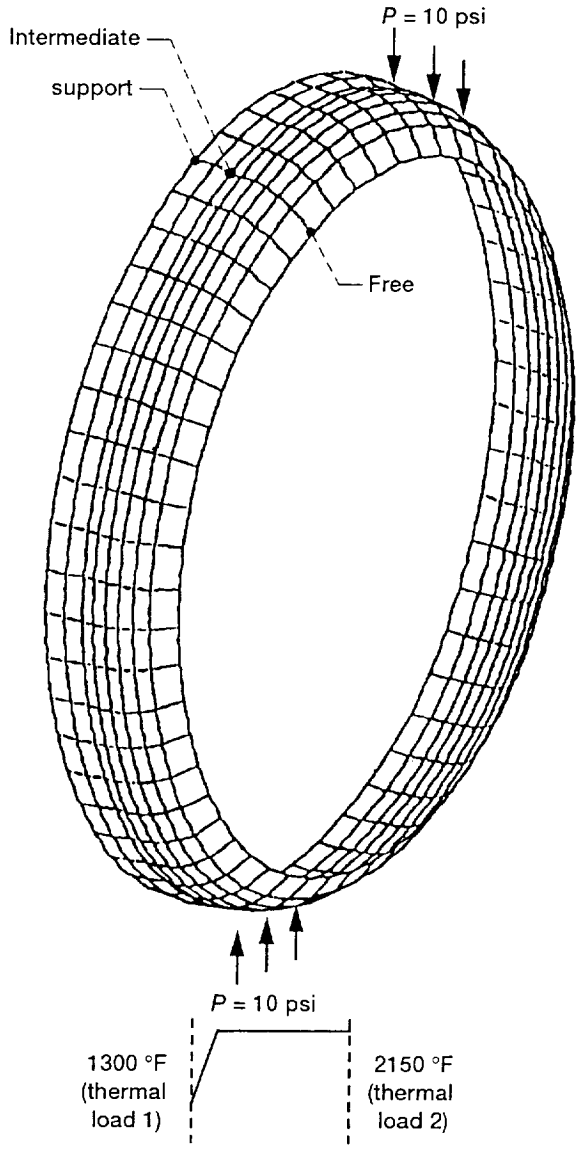

Figure 7.—Finite-element model for aircraft engine combustor liner.

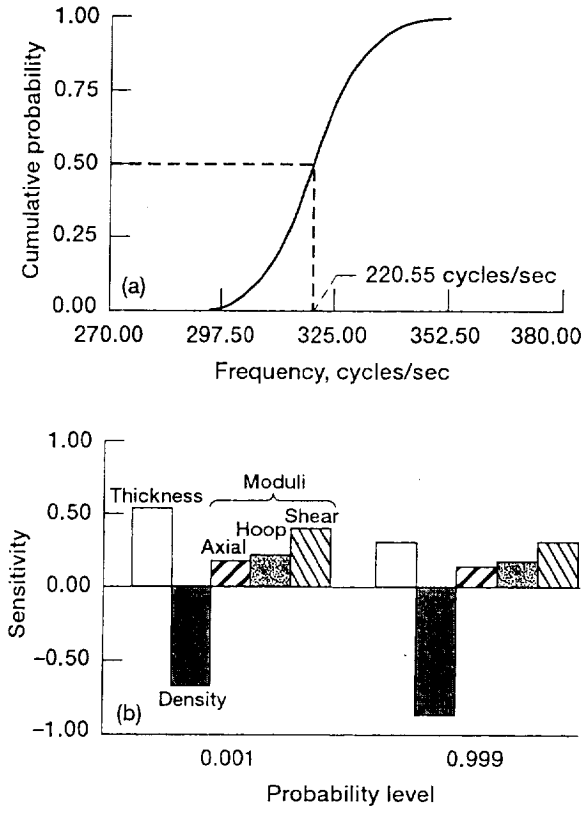

Figure 8.—Combustor liner probabilistic vibration frequency and sensitivities. (a) Cumulative distribution function of frequency. (b) Sensitivity factors.

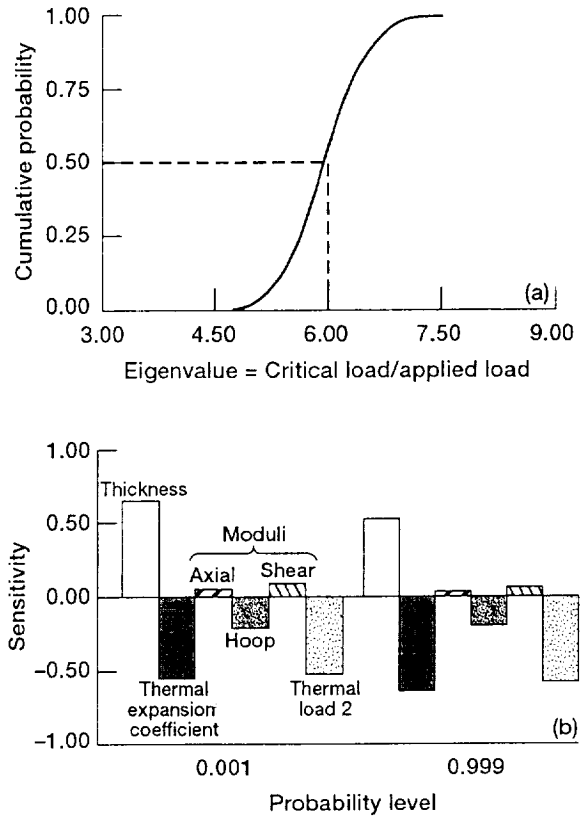

Figure 9.—Combustor liner probabilistic buckling and sensitivity. (a) Cumulative distribution function for buckling. (b) Sensitivity factors.

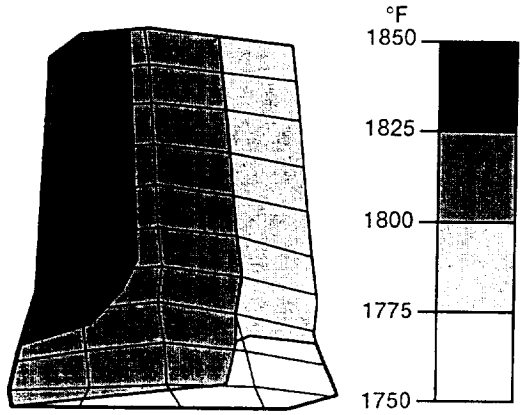

Temperature, °F

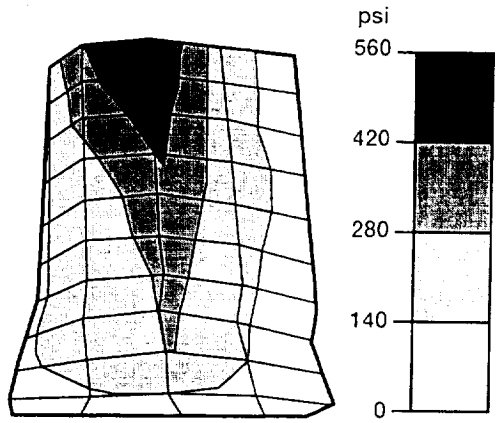

Pressure, psi

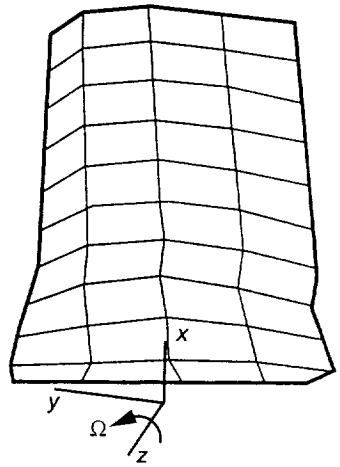

Centrifugal loads

Figure 10.—Finite-element model of space shuttle main engine blade with thermomechanical loads. Rotational speed, Ω, 40 000 rpm.

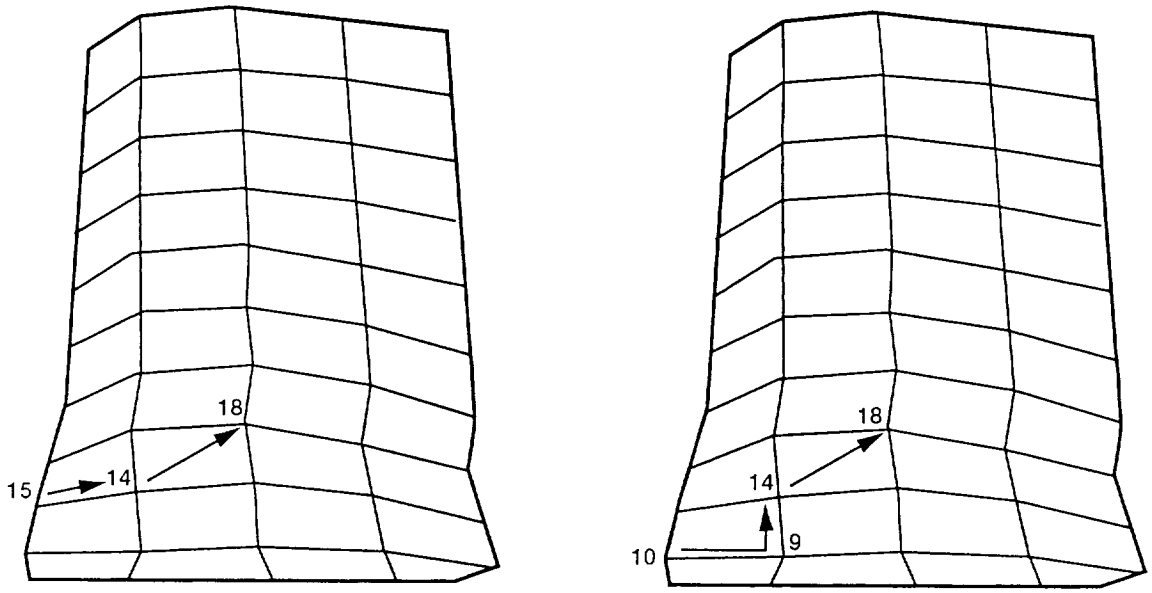

Path A
Probability that path A occurs, 0.00001

Path B
Probability that path B occurs, 0.0002

Figure 11.—Structural reliability of space shuttle main engine blade for 1 000 000 fatigue cycles and probable propagation paths to structural fracture. Blade geometry: 0.75 in. long by 1.0 in. wide at base.

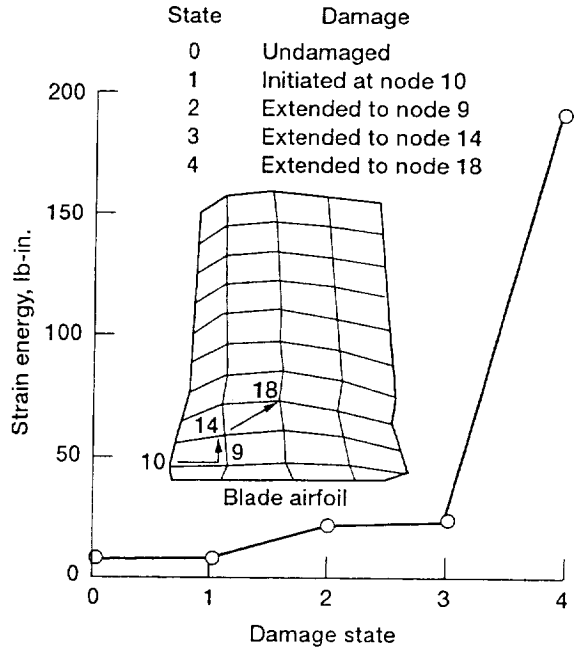

Figure 12.—Damage tolerance of space shuttle main engine blade along most probable progressive damage path leading to structural fracture.

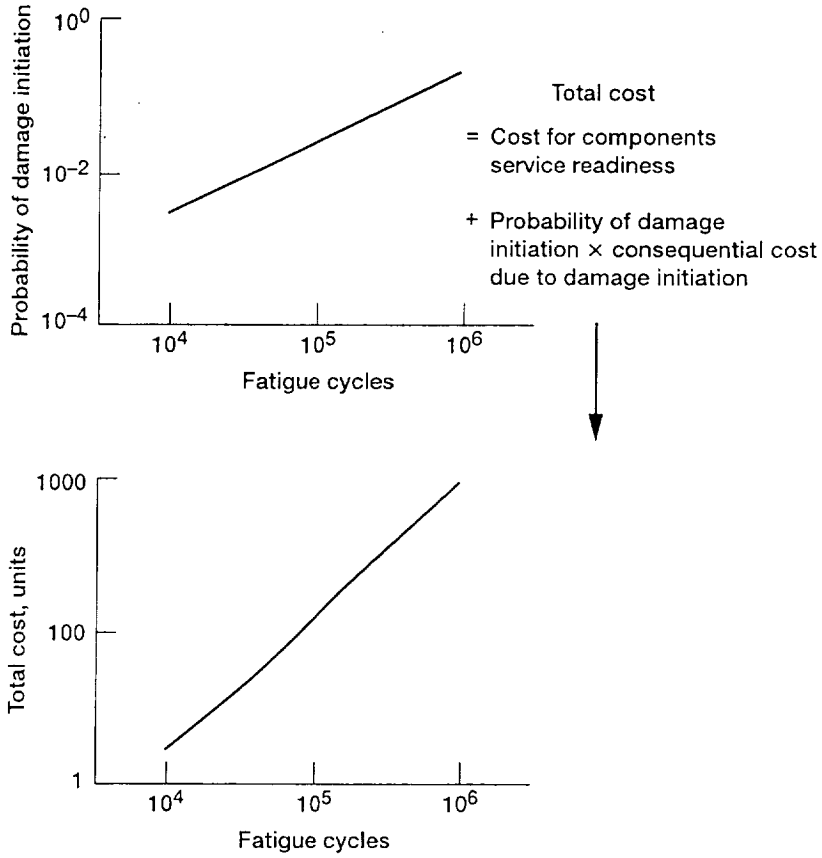

Figure 13.—Probabilistic risk-cost assessment of space shuttle main engine blade.

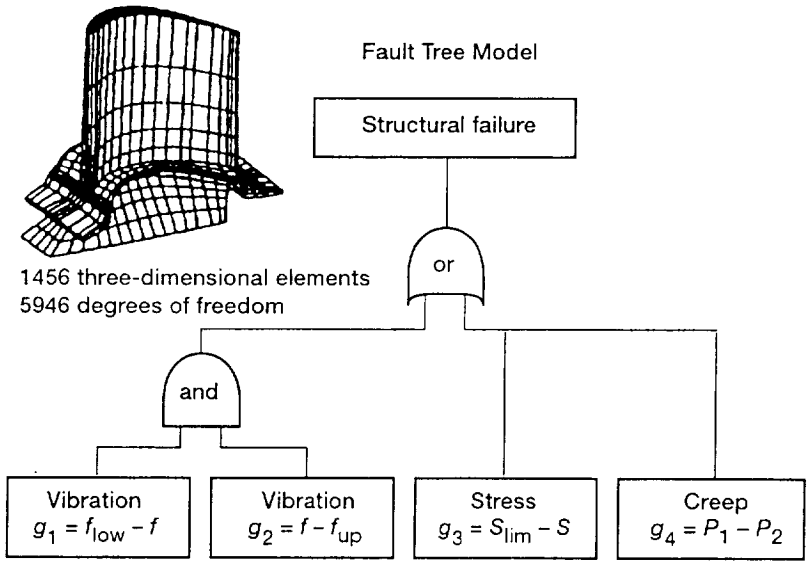

Figure 14.—System reliability using fault tree simulation. Failure occurs if $[g_1 < 0$ and $g_2 < 0]$ or $[g_3 < 0]$ or $[g_4 < 0]$. Finite-element model used for all bottom events.

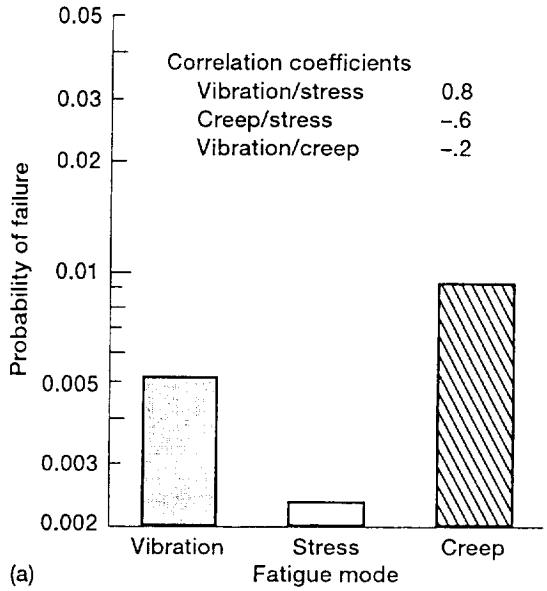

Figure 15.—System reliability using fault tree simulation and primitive variables sensitivities. (a) Failure mode. (b) Random variables. Creep coefficient, B_o.

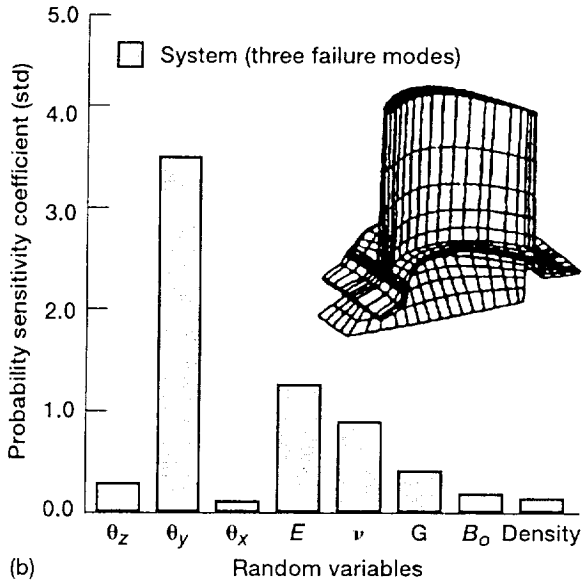

Figure 15.—Concluded. (b) Random variables. Creep coefficient, B_o.